Demixing and Remixing Kinetics of Poly(2-isopropyl-2-oxazoline) (PIPOZ) Aqueous Solutions Studied by Modulated Temperature Differential Scanning Calorimetry

ARTICLE *in* MACROMOLECULES · JULY 2010

Impact Factor: 5.8 · DOI: 10.1021/ma1012368

4 AUTHORS, INCLUDING:

Jun Zhao
National Center for Nanoscience and Techn…
84 PUBLICATIONS **831** CITATIONS
SEE PROFILE

Hoogenboom Richard
Ghent University
415 PUBLICATIONS **10,582** CITATIONS
SEE PROFILE

Guy Van Assche
Vrije Universiteit Brussel
129 PUBLICATIONS **1,791** CITATIONS
SEE PROFILE

Macromolecules
ARTICLE

Macromolecules **2010**, *43*, 6853–6860 **6853**
DOI: 10.1021/ma1012368

Demixing and Remixing Kinetics of Poly(2-isopropyl-2-oxazoline) (PIPOZ) Aqueous Solutions Studied by Modulated Temperature Differential Scanning Calorimetry

Jun Zhao,[†] Richard Hoogenboom,[‡,§] Guy Van Assche,[†] and Bruno Van Mele*[,†]

[†]*Physical Chemistry and Polymer Science, Department of Materials and Chemistry, Vrije Universiteit Brussel, Pleinlaan 2, 1050 Brussels, Belgium,* [‡]*Laboratory of Macromolecular Chemistry and Nanoscience, Eindhoven University of Technology, Den Dolech 2, 5612 AZ Eindhoven, The Netherlands, and* [§]*Supramolecular Chemistry Group, Department of Organic Chemistry, Ghent University, Krijgslaan 281 S4, 9000 Ghent, Belgium*

Received June 2, 2010; Revised Manuscript Received July 14, 2010

ABSTRACT: The demixing and remixing kinetics of aqueous solutions of poly(2-isopropyl-2-oxazoline) (PIPOZ) with four different chain lengths (number-average molar mass of 3300−13000 g mol^{-1}) is studied by means of modulated temperature differential scanning calorimetry (MTDSC) in both nonisothermal and quasi-isothermal modes. The nonisothermal measurements show that the aqueous solutions of all four PIPOZ samples follow the lower critical solution temperature (LCST) phase behavior. Both the LCST and the corresponding polymer weight fraction (f_w) decrease with increasing molar mass: 33.8 ± 0.1 °C at 29.8 wt % for 3300 g mol^{-1} shifts to 26.2 ± 0.1 °C at 19.8 wt % for 13000 g mol^{-1}. This typical type I phase behavior of aqueous solutions of PIPOZ is in contrast to the typical type II phase behavior of poly(*N*-isopropylacrylamide) (PNIPAM) which has isomeric repeat units. The demixing and remixing kinetics throughout the phase transition is studied by quasi-isothermal heat capacity measurements. Overall, the response for PIPOZ solutions is markedly faster than for PNIPAM solutions.

Introduction

Stimuli-responsive polymers remain at the center of interest in science and technology even though it has been the focus of intensive research over several decades.[1] These polymers respond to external stimuli in a controlled and reversible way. The external stimuli include light, electric or magnetic fields, mechanical deformation, and change of temperature, pH, or ionic strength. The stimuli-responsive polymers have found various applications in areas such as coatings, medicine, carrier materials for drugs, enzymes, and catalysts.

The most intensively studied thermo-responsive polymers are poly(*N*-isopropylacrylamide) (PNIPAM),[2−29] poly(*N*-vinylcaprolactam) (PVCL),[30−37] and poly(methylvinylether) (PMVE).[23,38−44] There are relatively fewer reported studies on poly(2-isopropyl-2-oxazoline) (PIPOZ),[45−52] which is isomeric in repeat unit to PNIPAM as shown in Figure 1. Aqueous solutions of these water-soluble polymers follow the lower critical solution temperature (LCST) phase behavior and exhibit demixing from a homogeneous to a heterogeneous state upon heating and remixing upon cooling at physiological temperatures, which can be interesting for biological and medical applications.[28] The demixing (coil-to-globule transition) of these solutions is attributed to the formation of intramolecular (polymer−polymer) hydrogen bonds and the breaking of intermolecular (polymer−water) hydrogen bonds, and vice versa for the remixing (globule-to-coil transition).[9,10]

Aqueous polymer solutions can be classified in different types of LCST phase behavior.[12,30,38−40,42,53] Type I represents the Flory−Huggins miscibility behavior. The position of the minimum shifts toward a lower temperature and a lower polymer concentration with increasing polymer molar mass. In the limit of infinite polymer molar mass, the critical concentration is zero at the Θ-temperature. For type II, the minimum is almost independent of the polymer molar mass and the critical concentration remains nonzero, even for infinite molar mass. Type III reveals two lower two-phase areas separated from one upper two-phase area at a specific temperature at which three phases are in equilibrium. The two minima have a different molar mass dependence. The minimum at a low concentration has a limiting critical concentration equal to zero for an infinite molar mass, as expected for classical Θ behavior (type I). The one at a higher concentration is independent of the molar mass (type II). The different types of phase behavior are highly related to the differences in the interaction between polymer segments and water molecules, and they can be modeled by the introduction of a polymer−solvent interaction function in the expression of the Flory−Huggins theory.[30] The strong dependence of the interaction parameter on the concentration could be the origin of type III phase behavior.[38] A typical example of a polymer showing type I behavior is PVCL,[30,33] while type II behavior is observed for PNIPAM.[12,19,27,29] PMVE displays type III phase behavior.[23,38,40−44] The full phase diagram of PIPOZ for a broad range of polymer concentrations has never been reported.

In recent years, we have studied the phase behavior and the demixing and remixing kinetics of aqueous polymer solutions using modulated temperature differential scanning calorimetry (MTDSC),[19,22,23,27,29,33,41,43,44] a powerful extension of conventional differential scanning calorimetry (DSC), in which a sinusoidal perturbation is superimposed on the underlying temperature program. MTDSC allows for the simultaneous measurement of heat flow, heat capacity, and heat flow phase. In the study of polymer materials using well-chosen MTDSC measuring conditions, the kinetic thermal processes, depending on time and absolute temperature, appear in the nonreversing heat flow

*To whom correspondence should be addressed. Telephone: +32-2-6293276. Fax: +32-2-6293278. E-mail: bvmele@vub.ac.be.

Published on Web 07/26/2010

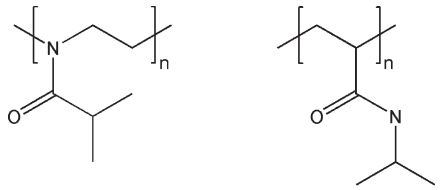

Figure 1. Chemical structures of poly(2-isopropyl-2-oxazoline) (PIPOZ) and poly(*N*-isopropylacrylamide) (PNIPAM).

(HF_{nonrev}), while properties with heat effects proportional to the heating rate are found in the reversing heat flow (HF_{rev}) or heat capacity (c_p) related signal. In this case, the HF_{rev} signal equals the average heating rate times the measured specific heat capacity (c_p), which is calculated as

$$c_p = \frac{A_{HF}}{A_T \omega} \quad (1)$$

where $A_T\omega$ is the amplitude of the imposed modulated heating rate, with A_T the temperature modulation amplitude, ω the modulation angular frequency ($=2\pi/p$), and p the modulation period; A_{HF} is the amplitude (of the first harmonic) of the resulting modulated heat flow. HF_{nonrev} equals the total heat flow (HF_{tot}) (the running average of the modulated signal) minus HF_{rev}. A complete description of the extraction of the heat capacity and other MTDSC signals can be found in the literature.[54−57]

This straightforward MTDSC deconvolution of c_p and thermal transformations in separate signals turned out to be very valuable for the study of the kinetics and chemo-rheology in reacting systems.[58−60] However, it is no longer valid for the characterization of fast processes, e.g., melting/crystallization,[61−65] temperature- or reaction-induced phase separation in blends[66−69] and phase separation in solutions.[19,22,23,27,29,33,41,43,44] Heat effects caused by these fast processes follow the modulated heating rate during each modulation cycle, and thus contribute to A_{HF} in eq 1 and to the c_p-signal derived from it. Hence, the c_p signal calculated by eq 1 contains a so-called excess contribution (c_p^{excess}) in addition to the baseline specific heat capacity (c_p^{base}), and is therefore called the apparent (specific) heat capacity.

$$c_p^{app}(T,t) = c_p^{base}(T) + c_p^{excess}(T,t) \quad (2)$$

c_p^{base} is based on thermodynamics and is (to a good approximation) only temperature-dependent. c_p^{excess} originates from the fast processes at the interface of coexisting phases and changes with the progress of the phase transformation, e.g. morphology development. As c_p^{excess} is temperature- and time-dependent, c_p^{app} is also temperature- and time-dependent and changes during the phase transformation.

MTDSC can be used to study the phase separation in both nonisothermal and quasi-isothermal (average heating rate equal to zero) conditions. For the nonisothermal measurements, during phase separation, the fast demixing/remixing processes following the applied temperature modulation will give rise to a c_p^{excess} superimposed on c_p^{base}. This feature enables the complete construction of the state diagram by means of nonisothermal c_p^{app} measurements.[19,22,23,27,29,33,41,43,44] For the quasi-isothermal measurements, the time-dependent behavior of c_p^{app} (and c_p^{excess}) in the phase separation region can provide additional information on the fast molecular processes of demixing and remixing (nanoscale miscibility) at the interface of coexisting phases and on the long-term evolution (slow processes) of this interface fraction toward an equilibrium condition (morphology development on a macroscopic level), which is independent of the thermal history and the phase separation kinetics.[19,22,27,29,33,41,44] Thus, the quasi-isothermal measurements make the real-time monitoring of temperature- or reaction-induced demixing and remixing possible.

In this work, the above-mentioned MTDSC concepts for aqueous solutions will be used to establish the state diagram and to investigate the demixing and remixing kinetics of aqueous solutions of PIPOZ with different molar masses over the full range of concentrations. A comparison with aqueous solutions of PNIPAM will be made to study the effect of the chemical structure.

Table 1. Characteristics of Poly(2-isopropyl-2-oxazoline)

polymer	M_0/I_0[a]	M_n[b] (g mol^{-1})	M_w/M_n[b]
PIPOZ 3K	25	3300	1.1
PIPOZ 6K	55	6200	1.1
PIPOZ 8K	100	7800	1.1
PIPOZ 13K	200	13 000	1.3

[a] Initial monomer/initiator feed ratio. [b] From size exclusion chromatography (SEC) measurements.

Experimental Section

Materials. PIPOZ with different molar masses and narrow distribution of molar mass (Table 1) were synthesized and purified similar to a procedure described elsewhere.[50,70] They are denoted here as PIPOZ 3K, 6K, 8K, and 13K. Water was deionized with a Millipore Milli-Q water purification system.

Solutions Preparation. Solution concentrations are expressed as weight fractions of PIPOZ (f_w). Starting from a dilute solution of PIPOZ in water with f_w of about 5 wt %, a full range of concentrations was prepared directly in TA Instruments T_{zero} hermetic aluminum crucibles of 40 μL. More concentrated solutions were prepared by drying the initial solution in air at ambient temperature to the target f_w, while more dilute solutions were prepared by diluting the initial solution with water to the target f_w. The final solutions for the subsequent MTDSC measurements had a mass of about 2.5 mg. All the hermetically sealed crucibles were put in the refrigerator horizontally with the lid side upward and kept at 4 °C for at least 24 h to obtain a homogeneous state. A few of the closed crucibles were perforated and the weight loss was measured at 100 °C using thermogravimetric analysis (TA Instruments Q5000 TGA) to check the preparation procedure (relative error of $f_w < 1.0\%$).

MTDSC Measurements. The MTDSC measurements were performed using a TA Instruments Q2000 DSC (T_{zero} DSC technique) with the MDSC option, equipped with an RCS cooling accessory and purged with nitrogen (50 mL min^{-1}). The instrument was calibrated in T4P mode, thus accounting for the heat transfer characteristics of the instrument and crucibles. Temperature and enthalpy were calibrated with indium. The hermetic crucibles were perforated for the measurements of pure PIPOZ. Standard modulation conditions with A_T of 0.5 K and p of 60 s were used. Scan rates were 1.0 and 2.5 K min^{-1} for phase separation measurements and glass transition measurements, respectively. For phase separation measurements, the solutions were kept isothermally for 30 min at a lower limit temperature of 2.0 °C and for 5 min at an upper limit temperature of 65.0 °C or higher (depending on f_w of the solutions). The same conditions were used for quasi-isothermal demixing and remixing experiments. The start point for quasi-isothermal demixing is reached by heating at 1.0 K min^{-1} from the homogeneous state at 2.0 °C, where the solutions were kept isothermally for 30 min. The start point of the quasi-isothermal remixing is reached by cooling at 1.0 K min^{-1} from the heterogeneous state at 65.0 °C after being kept isothermally for 5 min. For glass transition measurements, the solutions were kept isothermally for 10 min at a lower limit temperature of −90.0 °C and for 1 min at an upper limit temperature of 65.0 °C (or 100.0 °C for pure PIPOZ). The glass transition measurements were also used to observe the crystallization and melting of water. Three heating−cooling cycles

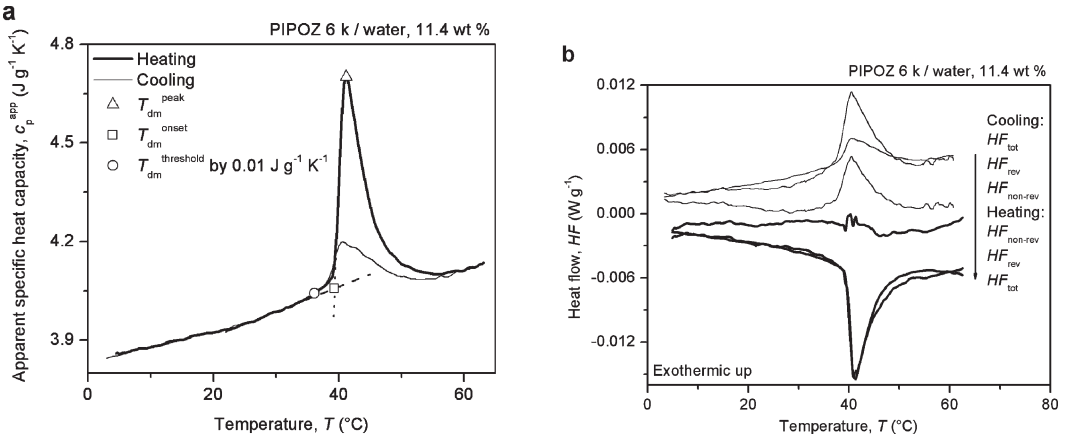

Figure 2. MTDSC c_p^{app} (a) and HF (b) traces for the nonisothermal demixing (heating, thick curves) and subsequent remixing (cooling, thin curves) of an aqueous solution of PIPOZ 6K with f_w of 11.4 wt %. In part a, T_{dm}^{peak}, T_{dm}^{onset}, and $T_{dm}^{threshold}$ by 0.01 J g^{-1} K^{-1} are shown. In part b, HF_{tot}, HF_{rev}, and HF_{nonrev} are given. All HF curves in part b are shifted vertically for clarity.

were run to control the reproducibility. For most measurements, all three cooling runs coincide very well. Only the first heating run was slightly different from the subsequent two heating runs, which might be due to sample preparation effects such as poor contact of fresh samples with crucible bottom. To reduce these effects, the second cycle was used for the analysis of the demixing and remixing, the second cooling was used for the analysis of the glass transition, while the first cooling and the second heating were used for the analysis of the crystallization and melting of water.

Results and Discussion

Nonisothermal Demixing and Remixing. MTDSC was used to study the nonisothermal demixing and remixing in aqueous solutions of PIPOZ. As an example, Figure 2 shows MTDSC results for the nonisothermal demixing (heating) and subsequent remixing (cooling) in aqueous solutions of PIPOZ 6K with weight fraction, f_w, of 11.4 wt %.

As for the aqueous solutions of PNIPAM, PVCL, and PMVE,[19,22,23,27,29,33,41,43,44] the demixing during heating is observed as a peak in c_p^{app} (Figure 2a), indicating a c_p^{excess} contribution arising from fast demixing/remixing processes following the applied temperature modulation. As before,[19] the demixing temperature is defined as the temperature at which c_p^{app} increases 0.01 J g^{-1} K^{-1} above the extrapolated baseline heat capacity (denoted as $T_{dm}^{threshold}$). Besides, the peak temperature of the demixing peak, T_{dm}^{peak}, and the onset temperature of the demixing peak, T_{dm}^{onset}, are also indicated in Figure 2a.

As shown in Figure 2a, for the aqueous PIPOZ 6K solution with f_w of 11.4 wt %, the area underneath the c_p^{app} curve during cooling (the remixing enthalpy) is much smaller than during the previous heating (the demixing enthalpy), which indicates that the remixing process is a slower process than the demixing, in accordance with our results on PNIPAM.[19] For temperatures outside the phase transition region, both c_p^{app} curves coincide.

In Figure 2b, the heat flow signals of the same MTDSC measurement are shown. The HF_{tot} signal corresponds to what would be observed in a conventional DSC measurement at the same heating rate. In heating, it shows an endothermic demixing (hydrogen bonds disruption between polymer segments and water molecules) starting near 35 °C and ending near 55 °C. In cooling, an exothermic remixing (hydrogen bonds formation between polymer segments and water molecules) occurs in the same temperature interval. It is worth noting that the remixing enthalpy obtained from HF_{tot}, written as ΔH_{rm}^{tot}, is the same (with opposite sign) as the demixing enthalpy ΔH_{dm}^{tot} obtained during the previous heating, within the uncertainty limits of ΔH (about 0.1 J g^{-1}), indicating that the demixing can be reversed on the time scale of the cooling run. In addition to HF_{tot}, its separation into the heat capacity based HF_{rev} and HF_{nonrev} is given in Figure 2b.

As a result of the different evolution of c_p^{app} (and thus of HF_{rev}) for heating and cooling, the separation of HF_{tot} into HF_{rev} and HF_{nonrev} also differs. During heating, almost the entire endothermic demixing peak can be seen in HF_{rev}; almost only the baseline is left in HF_{nonrev}. During the subsequent cooling, the exothermic remixing peak is distributed over both HF_{rev} and HF_{nonrev}. As HF_{rev} and c_p^{app} contain less noise than HF_{tot} and HF_{nonrev}, and as c_p^{app} can also be followed in quasi-isothermal conditions, both advantages of MTDSC over standard DSC,[54−57] the c_p^{app} signal will be primarily used for the discussion in this paper.

Figure 3 shows MTDSC c_p^{app} traces during the nonisothermal demixing (heating) and subsequent remixing (cooling) of aqueous PIPOZ solutions with four different molar masses over the whole range of concentrations. A single demixing peak can be seen for all the solutions with f_w below 75 wt %. For more concentrated solutions, no demixing peak can be seen. For temperatures outside the phase transition region, both heating and cooling c_p^{app} curves coincide. It is interesting to note that the demixing peak for all different polymers has almost the same shape, especially for f_w between 10 and 65 wt %: the demixing peak is always sharp on the low-temperature side and more gradually decaying on the high-temperature side. Compared to the demixing peak, the remixing peak is much smaller for f_w between 10 and 55 wt %. However, the remixing peak almost coincides with the demixing peak for other concentrations. The shape of the remixing peak is much more irregular than that of the demixing peak and even double remixing peaks can be seen for some concentrations. Compared to the demixing of a homogeneous solution, the remixing of the phase separated solution is less straightforward: the kinetics of the remixing process is often influenced by the thermal history of the sample and, more specifically, by the phase separated morphology formed previously.

Figure 4 summarizes the characteristic temperatures of the nonisothermal demixing shown in Figure 3: T_{dm}^{peak}, T_{dm}^{onset}, and $T_{dm}^{threshold}$ by 0.01 J g^{-1} K^{-1}. It can be seen that all these three different characteristic temperatures show that the aqueous PIPOZ solutions follow an LCST phase

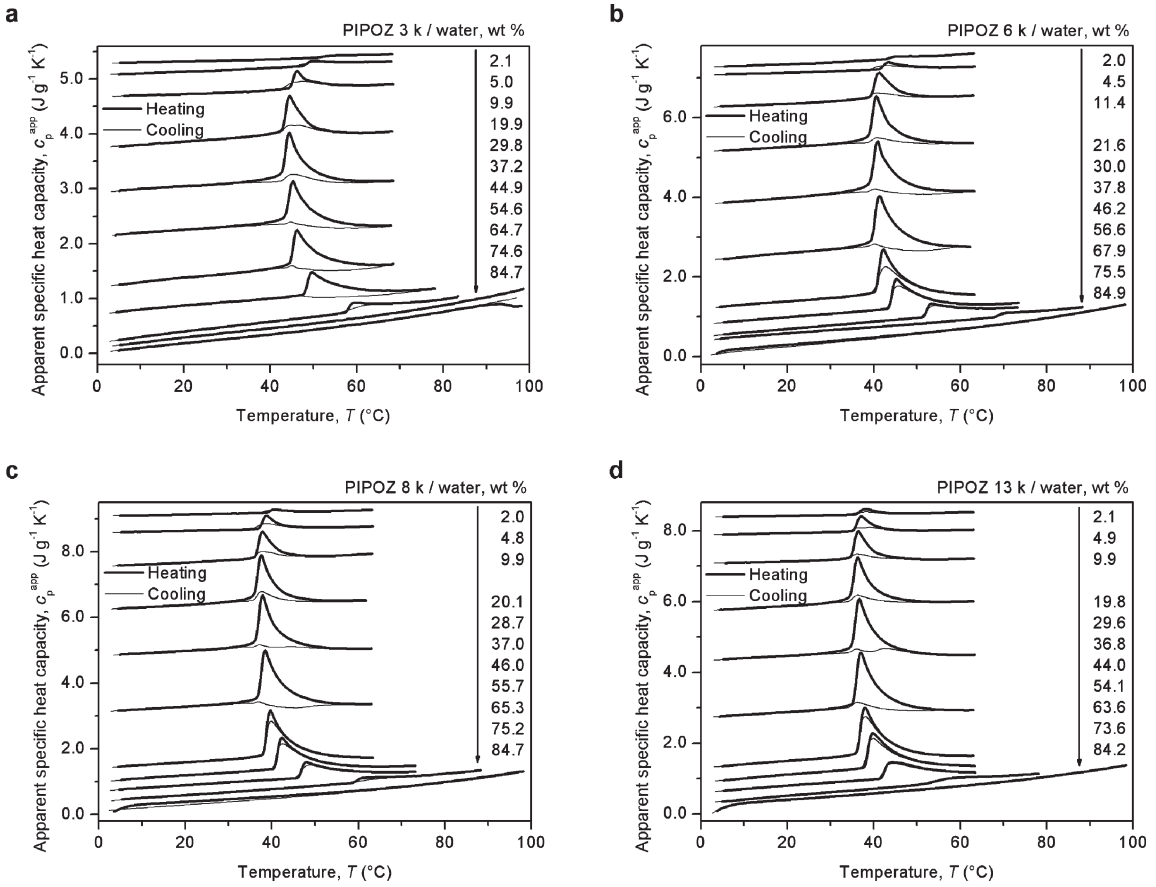

Figure 3. MTDSC c_p^{app} traces during nonisothermal demixing (heating, thick curves) and subsequent remixing (cooling, thin curves) in aqueous solutions of PIPOZ with different molar masses: 3K (a), 6K (b), 8K (c), and 13K (d). f_w is indicated beside each curve. All curves are shifted vertically for clarity, using the same shift for the heating and cooling curves of the same f_w.

behavior. Besides, the minimum slightly shifts to lower temperature with increasing molar mass (for $T_{dm}^{threshold}$ by 0.01 J g^{-1} K^{-1}: from 33.8 ± 0.1 °C at 29.8 wt % for 3300 g mol^{-1} to 26.2 ± 0.1 °C at 19.8 wt % for 13000 g mol^{-1}), which is a typical Type I phase behavior.[12,30,38−40,42,53] As a comparison, aqueous PNIPAM solutions follow typical type II behavior (the minimum is independent of the molar mass) although PIPOZ and PNIPAM possess isomeric repeat units.[19] A possible explanation might be the different ability to form hydrogen bonds between polymer segments and water molecules in the aqueous solution: relatively weaker hydrogen bonds are formed in PIPOZ solutions than in PNIPAM solutions, as PIPOZ has a tertiary amide in the main chain, while PNIPAM has a secondary amide, with an additional =NH− hydrogen bonding capacity, in the side group (see Figure 1).[71,72] An analogous argument seems valid for aqueous PVCL solutions, also showing Type I behavior; in the latter case PVCL contains a tertiary amide in the side group.[33] Although there is hydrophobic hydration for both PIPOZ and PNIPAM, this effect should not be significantly different for them because they have exactly the same isopropyl groups in side chains.[71,72]

Figure 5 shows the effect of f_w on the demixing enthalpy from c_p^{app}, ΔH_{dm}^{rev}, for aqueous solutions of PIPOZ. It can be seen that ΔH_{dm}^{rev} increases with decreasing f_w and levels off for the very low f_w. The maximum of ΔH_{dm}^{rev} for the dilute solutions of PIPOZ 13K is about 42.0 J (g polymer)$^{-1}$, which corresponds to about 4.7 kJ per mole of PIPOZ repeat units and is close to the energy required to break one hydrogen bond per polymer repeat unit.[15,17,73,74] For comparison, the PNIPAM with high molar mass has a value of ΔH_{dm}^{tot} (demixing enthalpy from HF_{tot}) of 5.5−7.5 kJ/mol of PNIPAM.[14,15,17,73,74] The decrease of ΔH_{dm}^{rev} with increasing f_w, especially for f_w above 20 wt %, is due to the decreasing hydration of the polymer segments. In more concentrated solutions, there are not enough water molecules to build up the full hydration structure around the polymer segments, which requires about 25 molecules per repeat unit, as estimated from the 20 wt % limit. At a fixed concentration, ΔH_{dm}^{rev} decreases with decreasing molar mass of PIPOZ. This is attributed to an increasing concentration of end groups.

Figure 6 shows MTDSC c_p^{app} traces for the cooling of concentrated aqueous PIPOZ 6K solutions and pure PIPOZ 6K. For the pure PIPOZ 6K, a well-defined glass transition can be seen at about 60 °C. As expected, the glass transition temperature, T_g, rapidly decreases with the addition of water. When f_w is decreased to below ca. 50 wt %, the crystallization of water cannot be avoided before reaching T_g, which makes accurate measurements of T_g impossible. It should be noted that all the solutions are cooled down from temperatures well below the demixing region and the homogeneous state is reached before the cooling run. Therefore, no effect of demixing on the observed glass transition should be expected. A similar glass transition behavior is observed for the other three PIPOZ solutions and pure PIPOZ samples (see Figure S1 in Supporting Information).

As an example, Figure 7 shows the state diagram of aqueous solutions of PIPOZ 6K by combining Figure 4 and the results from Figure 6 with additional data of T_c^{onset} (crystallization onset temperature) and T_m^{endset} (melting endset temperature) (see Figure S2 in the Supporting Information). The state diagrams of the other three PIPOZ

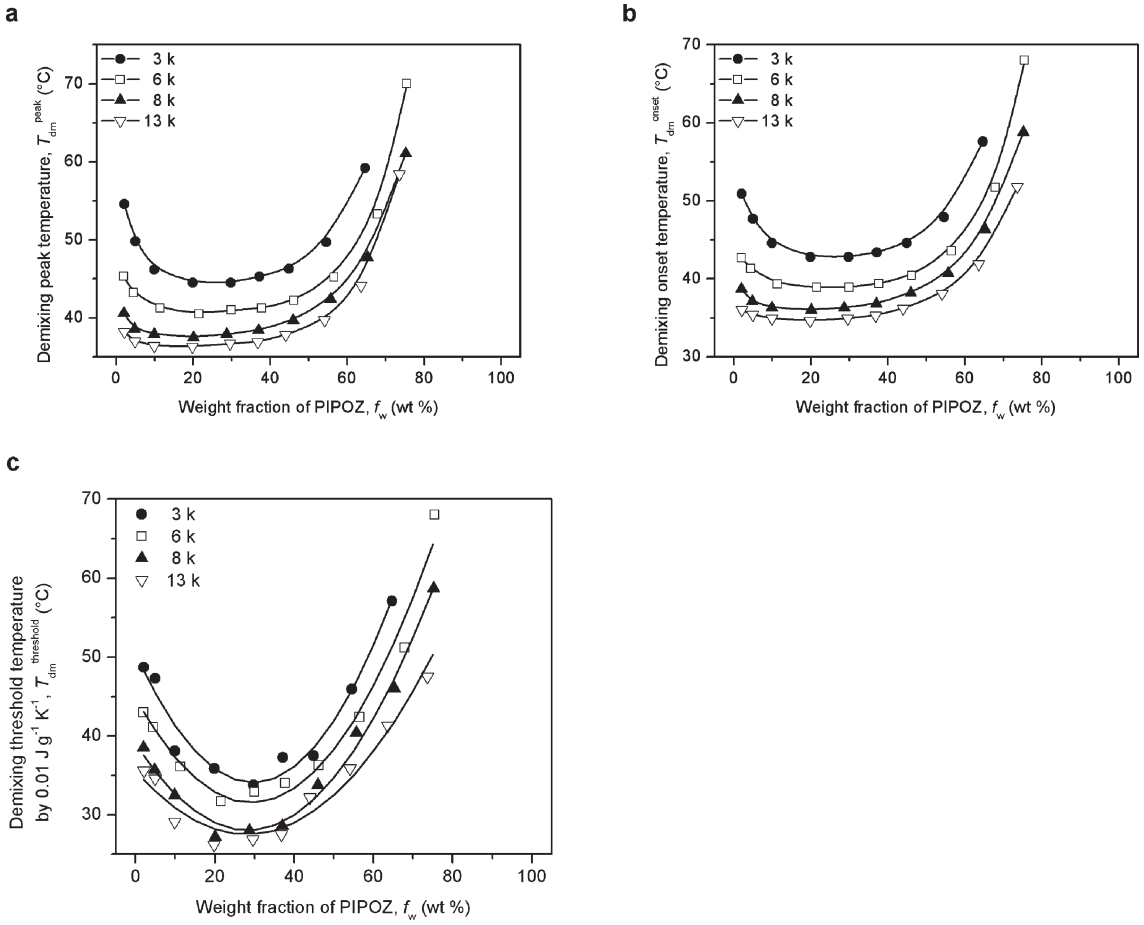

Figure 4. Effect of f_w on the demixing temperature for aqueous solutions of PIPOZ: T_{dm}^{peak} (a), T_{dm}^{onset} (b), and $T_{dm}^{threshold}$ by 0.01 J g^{-1} K^{-1} (c). Data are obtained from Figure 3.

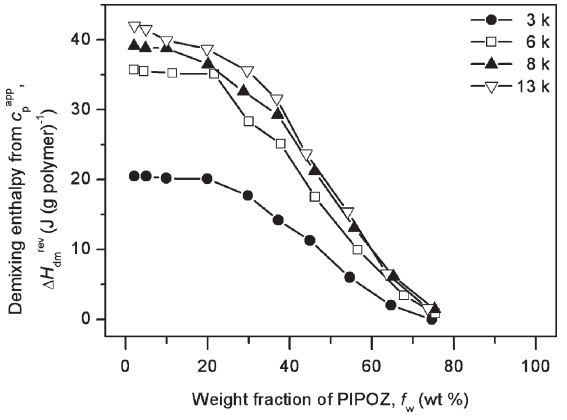

Figure 5. Effect of f_w on the demixing enthalpy from c_p^{app}, ΔH_{dm}^{rev}, for aqueous solutions of PIPOZ. Data are obtained from Figure 3.

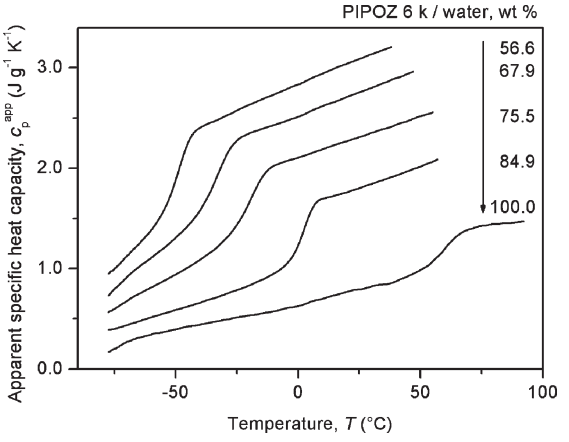

Figure 6. MTDSC c_p^{app} traces during cooling for the detection of T_g in concentrated aqueous solutions of PIPOZ 6K. f_w is indicated beside each curve. All curves are shifted vertically for clarity.

samples are quite similar. It can be seen that $T_{dm}^{threshold}$ is well above T_g and there is no intersection between them at any f_w, which is in contrast to the case of aqueous PNIPAM solutions.[19] For the latter, the intersection between $T_{dm}^{threshold}$ and T_g for the aqueous PNIPAM solutions results in a partial vitrification of the polymer-rich phase if the temperature is increased above the intersection temperature. For aqueous PIPOZ solutions, partial vitrification cannot happen because the polymer-rich phase formed after phase separation is always at temperatures well above its T_g.

Figure 7 also shows that both T_c^{onset} and T_m^{endset} of water decreases with increasing f_w due to the increasing solution viscosity (kinetic effect). The maxima of f_w to see T_c^{onset} and T_m^{endset} are ca. 46 and 57 wt %, respectively. Note that the limit of f_w for T_m^{endset} is higher than for T_c^{onset} due to a cold crystallization effect in the heating segment (see Figure S2b in Supporting Information). For the more concentrated solutions, the crystallization of water is too slow to occur on the time scale of the experiments, or even impossible, because the crystallization temperature would be too close to or below T_g.

Quasi-Isothermal Demixing and Remixing. Quasi-isothermal studies of the demixing and remixing kinetics are of particular

interest, as the c_p^{app} evolution during these quasi-isothermal experiments can be attributed to morphological developments in the solutions.[19,22,27,29,33,41,44] A decreasing c_p^{app} is indicating the exchange of a decreasing amount of material through the interface between the coexisting polymer-rich and water-rich phases in the reversible demixing/remixing process, as a result of a decreasing interfacial contact area or a decreasing interdiffusion rate (and vice versa).

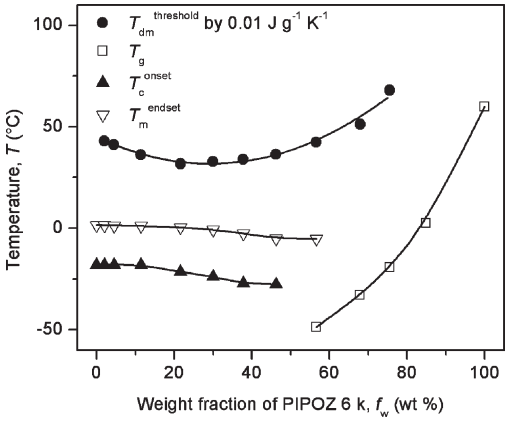

Figure 7. State diagram of aqueous solutions of PIPOZ 6K with $T_{dm}^{threshold}$ by 0.01 J g^{-1} K^{-1}, T_g, T_c^{onset}, and T_m^{endset}. $T_{dm}^{threshold}$ and T_g are obtained from Figures 3 and 6, respectively. T_c^{onset} and T_m^{endset} are obtained from Figure S2 in the Supporting Information.

Figure 8a shows an overlay of the evolution of c_p^{app} during quasi-isothermal demixing and remixing for aqueous PIPOZ 6K solutions with f_w of 30.0 wt %. Note that the start points of the quasi-isothermal demixing and remixing are always on the nonisothermal demixing and remixing curves, respectively. This is due to the fact that all start points are reached by the same temperature program as for the nonisothermal measurements. Figure 8b shows the same results, but focuses on narrower temperature interval for clarity. Figure 8c displays the corresponding time dependence of c_p^{app} during the quasi-isothermal demixing and remixing at five temperatures selected out of the temperature interval of Figure 8b. In nearly all cases, c_p^{app} levels off within 60 min. In experiments with quasi-isothermal segments of up to 1800 min at several temperatures in the phase transition region no further evolution of c_p^{app} was seen after 180 min.

For the temperatures close to T_{dm}^{peak} (41.0 °C), the largest quasi-isothermal evolutions in c_p^{app} are noted (Figure 8c). The evolution with time is much faster than for the aqueous PNIPAM solutions, for which more than a day is needed to reach the final state.[19] The much faster remixing of the PIPOZ solutions is mainly due to the absence of partial vitrification induced by demixing, which does occur in the

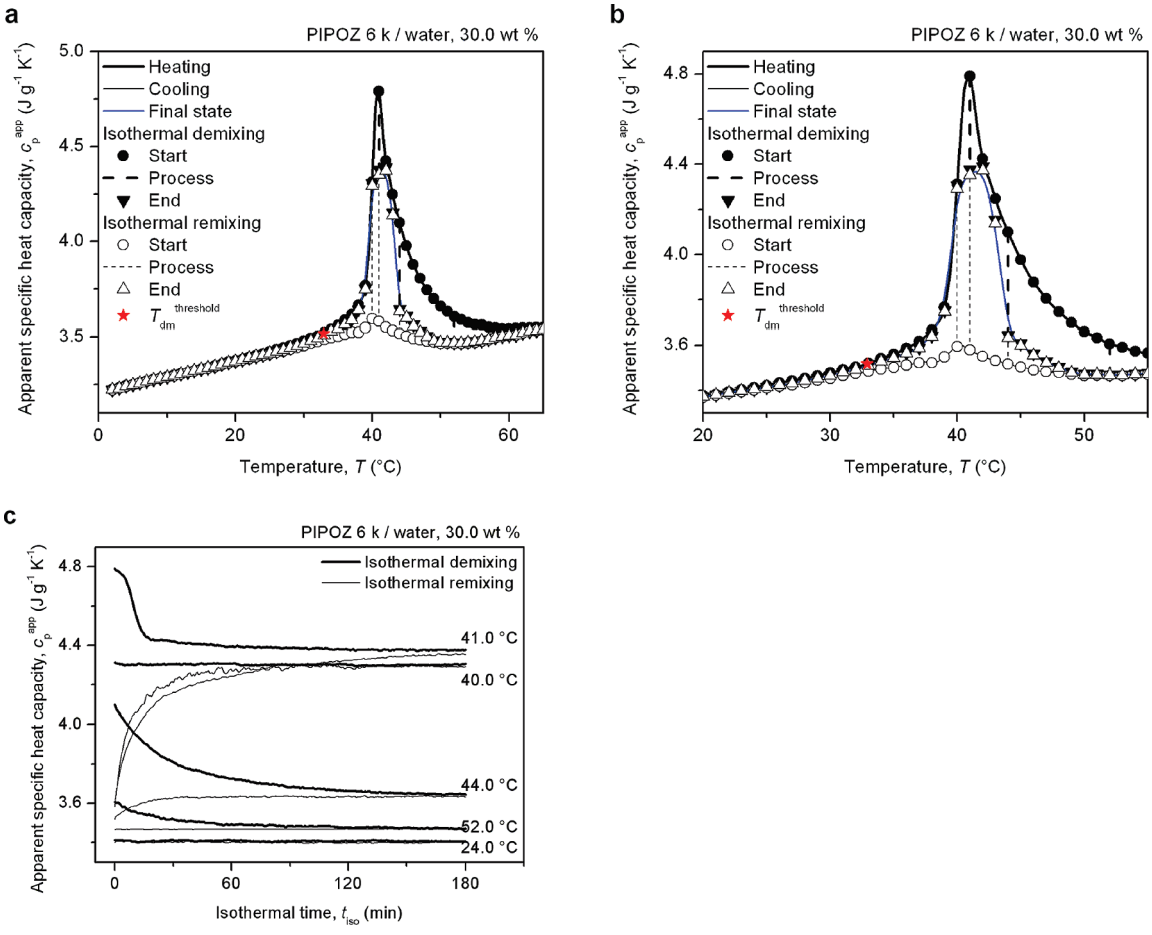

Figure 8. Quasi-isothermal demixing and remixing of aqueous PIPOZ 6K solutions with f_w of 30.0 wt %: c_p^{app} evolutions during quasi-isothermal demixing and remixing overlaid on the nonisothermal demixing (heating) and subsequent remixing (cooling) curves (a and b), and the time dependence of c_p^{app} during quasi-isothermal demixing (thick curves) and remixing (thin curves) (at 5 selected temperatures) (c). Part b is the same as part a, zooming in on a narrower temperature interval. The quasi-isothermal demixing and remixing processes and their start and end values obtained from part c are shown in parts a and b as vertical dashed lines and symbols, respectively. The final state trace in parts a and b is the average of the end values for the quasi-isothermal demixing and remixing at the same temperature (performed over the same temperature range as the nonisothermal measurements using an interval of 1.0 K).

PNIPAM solutions and strongly retards the diffusion of water into the polymer-rich phase.

As shown in Figure 8, for the PIPOZ 6K solutions, the end points of the quasi-isothermal demixing and remixing at a given temperature are always very close to each other, which indicates that the solution evolves to a final state (morphology) at that given temperature, independent of the thermal history. The final state curve is closer to the demixing curve for temperatures below T_{dm}^{peak} (41.0 °C) but closer to the remixing curve for temperatures above T_{dm}^{peak}. Remarkably, for temperatures up to 40.0 °C, on the rising side of the demixing peak and well above $T_{dm}^{threshold}$ by 0.01 J g^{-1} K^{-1} (32.9 °C), the final state curve coincides with the heating curve. Thus, for aqueous PIPOZ solutions time-independence is observed up to just 1.0 K below $T_{dm}^{threshold}$. In contrast, for aqueous PNIPAM solutions, c_p^{app} becomes time-dependent at temperatures just above $T_{dm}^{threshold}$.[19] As a matter of fact, the PIPOZ results rather tend toward the results for aqueous solutions of graft copolymer, PNIPAM-*g*-PEO (poly(ethylene oxide)), where a time-independent response was found over the full temperature interval.[27] The fast response of the latter system was attributed to the presence of the PEO grafts inside the PNIPAM domains, ensuring a fast transport of water even through a partially vitrified matrix. Hence, for the aqueous PIPOZ solutions, the lack of partial vitrification, or more generally, the larger difference between the phase separation temperature and T_g of the polymer-rich phase, and the relatively weaker hydrogen bonds might be the reasons for the faster demixing and remixing kinetics.

For the aqueous solutions of the other three PIPOZ samples, quite similar results of quasi-isothermal demixing and remixing can be seen (see Figure S3 in Supporting Information).

Conclusions

The demixing and remixing kinetics of aqueous solutions of PIPOZ with different molar masses was studied by means of MTDSC in both nonisothermal and quasi-isothermal modes. The solutions follow a typical type I LCST phase behavior, in contrast to the typical type II phase behavior of aqueous PNIPAM solutions although PIPOZ and PNIPAM have isomeric repeat units. This difference can be explained by their ability to form hydrogen bonds between polymer segments and water molecules in the solution: relatively weaker hydrogen bonds are formed in the solutions of PIPOZ than in the PNIPAM solutions, as the =N−H group present in PNIPAM and participating in the formation of hydrogen bonds is absent in PIPOZ. Overall, the thermal response for aqueous PIPOZ solutions is faster than for PNIPAM solutions, both for demixing and remixing, which is most likely due to the relatively weaker hydrogen bonding capacity of PIPOZ and the absence of partial vitrification of the polymer-rich phase during phase separation in the aqueous PIPOZ solutions.

Acknowledgment. Vrije Universiteit Brussel is grateful for financial support of the Research Foundation-Flanders (FWO-Vlaanderen; Project G.0214.05N). R.H. is grateful to The Netherlands Scientific Organisation (NWO) for financial support.

Supporting Information Available: Three figures showing MTDSC thermograms during cooling for the detection of T_g in concentrated aqueous solutions PIPOZ 3K, 8K, and 13K, MTDSC thermograms during cooling and subsequent heating for the detection of T_c^{onset} and T_m^{endset} in aqueous solutions of PIPOZ 6K, and an overlay of the c_p^{app} evolutions during quasi-isothermal demixing and remixing in aqueous PIPOZ 3K, PIPOZ 8K, and PIPOZ 13K solutions with f_w close to 30 wt %. This material is available free of charge via the Internet at http://pubs.acs.org.

References and Notes

(1) Winnik, F. M.; Whitten, D. G.; Urban, M. W.; Lopez, G. *Langmuir* **2007**, *23*, 1–2.
(2) Fujishige, S.; Kubota, K.; Ando, I. *J. Phys. Chem.* **1989**, *93*, 3311–3313.
(3) Winnik, F. M. *Macromolecules* **1990**, *23*, 233–242.
(4) Tokuhiro, T.; Amiya, T.; Mamada, A.; Tanaka, T. *Macromolecules* **1991**, *24*, 2936–2943.
(5) Schild, H. G. *Prog. Polym. Sci.* **1992**, *17*, 163–249.
(6) Tiktopulo, E. I.; Bychkova, V. E.; Ricka, J.; Ptitsyn, O. B. *Macromolecules* **1994**, *27*, 2879–2882.
(7) Moerkerke, R.; Koningsveld, R.; Berghmans, H.; Dusek, K.; Solc, K. *Macromolecules* **1995**, *28*, 1103–1107.
(8) Tiktopulo, E. I.; Uversky, V. N.; Lushchik, V. B.; Klenin, S. I.; Bychkova, V. E.; Ptitsyn, O. B. *Macromolecules* **1995**, *28*, 7519–7524.
(9) Wang, X.; Qiu, X.; Wu, C. *Macromolecules* **1998**, *31*, 2972–2976.
(10) Wu, C.; Wang, X. *Phys. Rev. Lett.* **1998**, *80*, 4092–4094.
(11) Lin, S.-Y.; Chen, K.-S.; Run-Chu, L. *Polymer* **1999**, *40*, 2619–2624.
(12) Afroze, F.; Nies, E.; Berghmans, H. *J. Mol. Struct.* **2000**, *554*, 55–68.
(13) Grinberg, V. Y.; Dubovik, A. S.; Kuznetsov, D. V.; Grinberg, N. V.; Grosberg, A. Y.; Tanaka, T. *Macromolecules* **2000**, *33*, 8685–8692.
(14) Kujawa, P.; Winnik, F. M. *Macromolecules* **2001**, *34*, 4130–4135.
(15) Avoce, D.; Liu, H. Y.; Zhu, X. X. *Polymer* **2003**, *44*, 1081–1087.
(16) Balamurugan, S.; Mendez, S.; Balamurugan, S. S.; O'Brien, M. J., II; Lopez, G. P. *Langmuir* **2003**, *19*, 2545–2549.
(17) Nichifor, M.; Zhu, X. X. *Polymer* **2003**, *44*, 3053–3060.
(18) Stieger, M.; Richtering, W. *Macromolecules* **2003**, *36*, 8811–8818.
(19) Van Durme, K.; Van Assche, G.; Van Mele, B. *Macromolecules* **2004**, *37*, 9596–9605.
(20) Okada, Y.; Tanaka, F. *Macromolecules* **2005**, *38*, 4465–4471.
(21) Kita, R.; Wiegand, S. *Macromolecules* **2005**, *38*, 4554–4556.
(22) Van Durme, K.; Van Mele, B.; Loos, W.; Du Prez, F. E. *Polymer* **2005**, *46*, 9851–9862.
(23) Van Durme, K.; Rahier, H.; Van Mele, B. *Macromolecules* **2005**, *38*, 10155–10163.
(24) Kujawa, P.; Segui, F.; Shaban, S.; Diab, C.; Okada, Y.; Tanaka, F.; Winnik, F. M. *Macromolecules* **2006**, *39*, 341–348.
(25) Cheng, H.; Shen, L.; Wu, C. *Macromolecules* **2006**, *39*, 2325–2329.
(26) Kujawa, P.; Tanaka, F.; Winnik, F. M. *Macromolecules* **2006**, *39*, 3048–3055.
(27) Van Durme, K.; Van Assche, G.; Aseyev, V.; Raula, J.; Tenhu, H.; Van Mele, B. *Macromolecules* **2007**, *40*, 3765–3772.
(28) Vertommen, M. A. M. E.; Cornelissen, H.-J. L.; Dietz, C. H. J. T.; Hoogenboom, R.; Kemmere, M. F.; Keurentjes, J. T. F. *J. Membr. Sci.* **2008**, *322*, 243–248.
(29) Zhao, J.; Shan, J.; Van Assche, G.; Tenhu, H.; Van Mele, B. *Macromolecules* **2009**, *42*, 5317–5327.
(30) Meeussen, F.; Nies, E.; Berghmans, H.; Verbrugghe, S.; Goethals, E.; Du Prez, F. *Polymer* **2000**, *41*, 8597–8602.
(31) Laukkanen, A.; Hietala, S.; Maunu, S. L.; Tenhu, H. *Macromolecules* **2000**, *33*, 8703–8708.
(32) Maeda, Y.; Nakamura, T.; Ikeda, I. *Macromolecules* **2002**, *35*, 217–222.
(33) Van Durme, K.; Verbrugghe, S.; Du Prez, F. E.; Van Mele, B. *Macromolecules* **2004**, *37*, 1054–1061.
(34) Laukkanen, A.; Valtola, L.; Winnik, F. M.; Tenhu, H. *Macromolecules* **2004**, *37*, 2268–2274.
(35) Okhapkin, I. M.; Bronstein, L. M.; Makhaeva, E. E.; Matveeva, V. G.; Sulman, E. M.; Sulman, M. G.; Khokhlov, A. R. *Macromolecules* **2004**, *37*, 7879–7883.
(36) Laukkanen, A.; Winnik, F. M.; Tenhu, H. *Macromolecules* **2005**, *38*, 2439–2448.
(37) Kharlampieva, E.; Pristinski, D.; Sukhishvili, S. A. *Macromolecules* **2007**, *40*, 6967–6972.
(38) Schaefer-Soenen, H.; Moerkerke, R.; Berghmans, H.; Koningsveld, R.; Dusek, K.; Solc, K. *Macromolecules* **1997**, *30*, 410–416.
(39) Moerkerke, R.; Meeussen, F.; Koningsveld, R.; Berghmans, H.; Mondelaers, W.; Schacht, E.; Dusek, K.; Solc, K. *Macromolecules* **1998**, *31*, 2223–2229.

(40) Meeussen, F.; Bauwens, Y.; Moerkerke, R.; Nies, E.; Berghmans, H. *Polymer* **2000**, *41*, 3737–3743.
(41) Swier, S.; Van Durme, K.; Van Mele, B. *J. Polym. Sci., Part B: Polym. Phys.* **2003**, *41*, 1824–1836.
(42) Nies, E.; Ramzi, A.; Berghmans, H.; Li, T.; Heenan, R. K.; King, S. M. *Macromolecules* **2005**, *38*, 915–924.
(43) Van Durme, K.; Van Mele, B.; Bernaerts, K. V.; Verdonck, B.; Du Prez, F. E. *J. Polym. Sci., Part B: Polym. Phys.* **2006**, *44*, 461–469.
(44) Van Durme, K.; Van Assche, G.; Nies, E.; Van Mele, B. *J. Phys. Chem. B* **2007**, *111*, 1288–1295.
(45) Uyama, H.; Kobayashi, S. *Chem. Lett.* **1992**, 1643–1646.
(46) Diab, C.; Akiyama, Y.; Kataoka, K.; Winnik, F. M. *Macromolecules* **2004**, *37*, 2556–2562.
(47) Park, J.-S.; Akiyama, Y.; Winnik, F. M.; Kataoka, K. *Macromolecules* **2004**, *37*, 6786–6792.
(48) Park, J.-S.; Kataoka, K. *Macromolecules* **2007**, *40*, 3599–3609.
(49) Demirel, A. L.; Meyer, M.; Schlaad, H. *Angew. Chem., Int. Ed.* **2007**, *46*, 8622–8624.
(50) Hoogenboom, R.; Thijs, H. M. L.; Jochems, M. J. H. C.; Van Lankvelt, B. M.; Fijten, M. W. M.; Schubert, U. S. *Chem. Commun.* **2008**, *44*, 5758–5760.
(51) Hoogenboom, R. *Angew. Chem., Int. Ed.* **2009**, *48*, 7978–7994.
(52) Bloksma, M. M.; Bakker, D. J.; Webber, C.; Hoogenboom, R.; Schubert, U. S. *Macromol. Rapid Commun.* **2010**, *31*, 724–728.
(53) Solc, K.; Dusek, K.; Koningsveld, R.; Berghmans, H. *Collect. Czech. Chem. Commun.* **1995**, *60*, 1661–1688.
(54) Reading, M. *Trends Polym. Sci.* **1993**, *8*, 248–253.
(55) Wunderlich, B.; Jin, Y.; Boller, A. *Thermochim. Acta* **1994**, *238*, 277–293.
(56) Reading, M.; Luget, A.; Wilson, R. *Thermochim. Acta* **1994**, *238*, 295–307.
(57) *Modulated-Temperature Differential Scanning Calorimetry: Theoretical and Practical Applications in Polymer Characterization* (*Hot Topics in Thermal Analysis and Calorimetry*); Reading, M., Hourston, D. J., Eds.; Springer: London, 2006.
(58) Van Assche, G.; Van Hemelrijck, A.; Rahier, H.; Van Mele, B. *Thermochim. Acta* **1995**, *268*, 121–142.
(59) Swier, S.; Van Mele, B. *J. Polym. Sci., Part B: Polym. Phys.* **2003**, *41*, 594–608.
(60) Swier, S.; Van Mele, B. *Macromolecules* **2003**, *36*, 4424–4435.
(61) Ishikiriyama, K.; Wunderlich, B. *J. Polym. Sci., Part B: Polym. Phys.* **1997**, *35*, 1877–1886.
(62) Minakov, A. A.; Schick, C. *Thermochim. Acta* **1999**, *330*, 109–119.
(63) Miltner, H. E.; Rahier, H.; Pozsgay, A.; Pukanszky, B.; Van Mele, B. *Compos. Interface.* **2005**, *12*, 787–803.
(64) Miltner, H. E.; Van Assche, G.; Pozsgay, A.; Pukanszky, B.; Van Mele, B. *Polymer* **2006**, *47*, 826–835.
(65) Zhao, J.; Swinnen, A.; Van Assche, G.; Manca, J.; Vanderzande, D.; Van Mele, B. *J. Phys. Chem. B* **2009**, *113*, 1587–1591.
(66) Dreezen, G.; Groeninckx, G.; Swier, S.; Van Mele, B. *Polymer* **2001**, *42*, 1449–1459.
(67) Swier, S.; Pieters, R.; Van Mele, B. *Polymer* **2002**, *43*, 3611–3620.
(68) Swier, S.; Van Mele, B. *Polymer* **2003**, *44*, 2689–2699.
(69) Pieters, R.; Miltner, H. E.; Van Assche, G.; Van Mele, B. *Macromol. Symp.* **2006**, *233*, 36–41.
(70) Hoogenboom, R.; Fijten, M. W. M.; Thijs, H. M. L.; Van Lankvelt, B. M.; Schubert, U. S. *Des. Monomers Polym.* **2005**, *8*, 659–671.
(71) Tamai, Y.; Tanaka, H.; Nakanishi, K. *Macromolecules* **1996**, *29*, 6750–6760.
(72) Tamai, Y.; Tanaka, H.; Nakanishi, K. *Macromolecules* **1996**, *29*, 6761–6769.
(73) Schild, H. G.; Tirrell, D. A. *J. Phys. Chem.* **1990**, *94*, 4352–4356.
(74) Israelachvili, J. N. *Intermolecular and Surface Forces*; Academic Press: London, U.K., 1992.